

# A data-driven partitioned approach for the resolution of time-dependent optimal control problems with dynamic mode decomposition

Eleonora Donadini\*, Maria Strazzullo†, Marco Tezzele‡ and Gianluigi Rozza§

Mathematics Area, mathLab, SISSA, via Bonomea 265, I-34136 Trieste, Italy

November 30, 2021

## Abstract

This work recasts time-dependent optimal control problems governed by partial differential equations in a Dynamic Mode Decomposition with control framework. Indeed, since the numerical solution of such problems requires a lot of computational effort, we rely on this specific data-driven technique, using both solution and desired state measurements to extract the underlying system dynamics. Thus, after the Dynamic Mode Decomposition operators construction, we reconstruct and perform future predictions for all the variables of interest at a lower computational cost with respect to the standard space-time discretized models. We test the methodology in terms of relative reconstruction and prediction errors on a boundary control for a Graetz flow and on a distributed control with Stokes constraints.

## Contents

<b>1</b>	<b>Introduction</b>	<b>1</b>
<b>2</b>	<b>Time-dependent optimal control problems</b>	<b>2</b>
<b>3</b>	<b>Dynamic mode decomposition with control</b>	<b>3</b>
<b>4</b>	<b>A partitioned approach for time-dependent OCPs</b>	<b>4</b>
<b>5</b>	<b>Numerical results</b>	<b>4</b>
5.1	Boundary OCP governed by a Graetz Flow . . . . .	5
5.2	OCP governed by time-dependent Stokes Equations . . . . .	5
<b>6</b>	<b>Conclusions and perspectives</b>	<b>7</b>

## 1 Introduction

Scientific and industrial contexts need to represent natural phenomena through mathematical models. Historically, this role has been played by partial differential equations (PDEs) and by their numerical simulations. Yet, the model equations, in some frameworks, are not enough to well describe the complexity of the natural phenomenon one is dealing with. To increase the reliability of a proposed PDEs-based model, a very classical and elegant mathematical tool has been exploited: optimal control. This technique responds to the need for reducing the gap between PDEs and collected data. Indeed, the data information, given by some previous knowledge on the system, is exploited in order to achieve a *desired configuration*: a convenient profile similar to

---

\*edonadini@sissa.it

†maria.strazzullo@sissa.it

‡marco.tezzele@sissa.it

§gianluigi.rozza@sissa.it

the behaviour observed or expected in nature. Namely, through a PDE-constrained minimization strategy, optimal control problems (OCPs) are able to steer the solution of the problem at hand towards a target profile. OCPs governed by PDEs are widespread in many scientific applications: some examples in shape optimization may be found in [9, 14, 23] or, in fluid dynamics, in [7, 8, 25] where a parametrized setting is discussed. In the same framework, we can cite biomedical applications [3, 20, 37, 44], or environmental ones [27, 28, 33, 35]. From these references, it is clear that OCPs are of indisputable usefulness in many applications. Yet, they still are very complex to analyse and to simulate, most of all if time-dependency is taken into consideration, since it requires larger computational costs. Despite these difficulties, time-dependent OCPs have been treated in many works: here a far from exhaustive list [15, 18, 21, 31, 32, 34, 36, 35]. In contrast with the aforementioned works, we tackle the study of the evolution of OCPs through the employment of dynamic mode decomposition with control (DMDC) [26], which is a data-driven technique for system identification in the context of feedback and control. The idea is to use the desired state from the OCPs framework as forcing term within the DMDC. Then, with a partitioned approach, we use the solution snapshots to construct different DMDC operators. With such operators, given new actuation snapshots, we perform future predictions for all the variables of interest, in a data-driven fashion. This results in great advantages in terms of computational time, keeping the accuracy within a certain threshold, as usual in the reduced order modeling framework [29]. The main novelty of this work, thus, is the recasting of an OCP in a DMDC framework: to the best of our knowledge, indeed, this is the first time that it is highlighted and investigated. We propose two test cases: a boundary control governed by a Graetz flow and a distributed control with Stokes constraints.

## 2 Time-dependent optimal control problems

We provide the continuous formulation for general time dependent OCP. Let us consider the spatial domain  $\Omega \subset \mathbb{R}^d$ , with  $d = 2, 3$ : here, the analysed physical phenomenon, described by a linear time-dependent PDE, is taking place in the time interval  $[0, T]$ . Furthermore, we denote with  $\Gamma_D$  and  $\Gamma_N$  two non-overlapping boundary portions where homogeneous Dirichlet and Neumann boundary conditions apply. In the context of constrained optimization, we consider an Hilbert space  $Y$  such that  $Y \hookrightarrow H \hookrightarrow Y^*$  for some suitable  $H$ . Moreover, we define  $\mathcal{Y}_t = \{y \in L^2(0, T; Y) \text{ such that } y_t \in L^2(0, T; Y^*) \text{ with } y(t) = 0\} \subset \mathcal{Q}$ , with  $\mathcal{Q} = L^2(0, T; Y)$ . The problem *state variable*  $y$  is sought in  $\mathcal{Y}_0$ . In addition, we need to define  $\mathcal{U} = L^2(0, T; U)$  as the space for the *control variable*  $u$ , with  $U$  another suitable Hilbert space. The control acts on  $\Omega_u \subseteq \Omega$  of a portion of its boundary, say  $\Gamma_C \subset \partial\Omega$  with  $\Gamma_C \cap \Gamma_N \cap \Gamma_D = \emptyset$  while  $\Gamma_D \cup \Gamma_N \cup \Gamma_C = \partial\Omega$ . In the first case, we say that the control problem is *distributed*, while in the second case, we say that the problem is a *boundary control*. With no distinctions, from now on, we will call  $\Omega_u$  or  $\Gamma_C$  the *control domain*. In order to change the classical solution behaviour, we need to define a *controlled system* of the following form, for all  $q$  in  $\mathcal{Q}$ , considering once again  $y_0$  as initial condition

$$\int_0^T \langle y_t, q \rangle_{Y^*, Y} dt + \int_0^T a(y, q) dt = \int_0^T c(u, q) dt + \int_0^T \langle G, q \rangle_{Y^*, Y} dt, \quad (1)$$

with initial condition  $y_0$  where,  $a : Y \times Y \rightarrow \mathbb{R}$  is a coercive and continuous bilinear form and  $G \in Y^*$  represents the forcing and the boundary terms of the problem at hand, and  $c : U \times Y \rightarrow \mathbb{R}$  is the  $L^2$  product on the control domain. For the sake of notation, we define the controlled equation as  $\mathcal{E} : (\mathcal{Y} \times \mathcal{U}) \times \mathcal{Q} \rightarrow \mathbb{R}$ . Namely, (1) is verified when  $\mathcal{E}((y, u), q) = 0$  for all  $q$  in  $\mathcal{Q}$ . The goal of an OCP is to steer the solution towards a desired profile  $y_d \in \mathcal{Z} \supseteq \mathcal{Y}$  by minimizing a convex *cost functional*  $J : \mathcal{Y}_0 \times \mathcal{U} \rightarrow \mathbb{R}$  over  $\mathcal{Y}_0 \times \mathcal{U}$  such that (1) is verified. The functional  $J(y, u)$  must be defined case by case. For the well-posedness of the problem, the interested reader may refer to [17]. The minimization problem can be recast in an unconstrained fashion exploiting a Lagrangian approach [17, 40]. Thus, let us consider an arbitrary *adjoint variable*  $z \in \mathcal{Y}_T \subset \mathcal{Q}$  and define the following Lagrangian functional  $\mathcal{L}(y, u, z) = J(y, u) + \mathcal{E}((y, u), z)$ . It is well known in literature [17], that the aforementioned minimization of problem is equivalent to the following system: find  $(y, u, z) \in \mathcal{Y}_0 \times \mathcal{U} \times \mathcal{Y}_T$  such that

$$\begin{cases} D_y \mathcal{L}(y, u, z)[\omega] = 0 & \forall \omega \in \mathcal{Q} & \text{(adjoint equation),} \\ D_u \mathcal{L}(y, u, z)[\kappa] = 0 & \forall \kappa \in \mathcal{U} & \text{(optimality equation),} \\ D_z \mathcal{L}(y, u, z)[\zeta] = 0 & \forall \zeta \in \mathcal{Q} & \text{(state equation).} \end{cases} \quad (2)$$

In this context, the terms  $D_y, D_u$  and  $D_z$  will denote the differentiation with respect to the state, the control and the adjoint variables. We underline that, over the control domain, the optimality equation in strong form reads:

$$\alpha u - z = 0, \quad (3)$$

where the role of  $\alpha$  will be clarified in the next sections. We decided to solve (2) using a *space-time discretization*. The space-time techniques have been successfully applied in many contexts, from parabolic equations [12, 41, 42, 43] to time-dependent PDE-constrained optimization [15, 16, 34, 35, 36]. For the sake of brevity, we are not presenting the details of such an approach. The main idea is to treat the three-equations system (2) as a steady one, where all the time instances are sought all-at-once by means of a direct solver. The reader may refer to the previous cited bibliography for an insight to the method. For our purposes, it is enough to define a time discretization over  $[0, T]$  divided in  $N_t$  sub-intervals. Namely, we consider  $\Delta t > 0$  and the time instance  $t_k = k\Delta t$  for  $k = 0, \dots, N_t$ . Let us focus on the state, adjoint and control variables evaluated at  $t_k$ . At each  $t_k$ , the variables can be expressed through the corresponding spatial bases, in our case Finite Element (FE) bases. From now on, for the sake of notation,  $y_k$  will denote the column vector of FE coefficients of the FE expansion. The same argument applies to control and adjoint variables at  $t_k$ , denoted by  $u_k$  and  $p_k$ . We remark that state and adjoint have been discretized with the same discretized function space [34] to guarantee the well-posedness of the problem (2). To simulate the solution of the OCP we solve a system of dimension  $N_t(2\mathcal{N}_y + \mathcal{N}_u) \times N_t(2\mathcal{N}_y + \mathcal{N}_u)$  through a direct solver. This may lead to time consuming simulations to understand the field dynamic. To lighten these computational costs, one may use multigrid approaches combined with proper preconditioners, see e.g. [4, 30, 32] and the references therein. However, these iterative methods might only partially solve this issue. DMD-based techniques respond to the need of a fast prediction tool to avoid a complete simulation over the time interval  $[0, T]$ .

### 3 Dynamic mode decomposition with control

Dynamic mode decomposition (DMD) is a powerful method to identify and approximate dynamical systems using only few spatiotemporal coherent structures [5, 19]. It is ideally suited for time-dependent problems, and its data-driven nature makes it very versatile, also in industrial contexts [10, 38, 39].

When dealing with actuated systems, unfortunately, DMD fails to properly reconstruct the underlying dynamics since it is incapable of incorporating the contribution of the forcing term. To this end, dynamic mode decomposition with control (DMDC) [26] has been developed to overcome this issue. By including the actuation snapshots in the analysis it is able to provide reduced order representations for input-output systems. The DMDC method quantifies the effect of control inputs on the state of the system and computes the underlying dynamics without being confounded by the effect of external control. Recently, an extension for quantum control problems, called bilinear DMD, has been proposed in [13]. A local version of DMDC for predictive control of hydraulic fracturing can be found in [24], while for compressive system identification see [2].

Let us denote the snapshot representing the state of a system at the  $i$ -th time instant with  $x_i \in \mathbb{R}^{\mathcal{N}}$ , where  $\mathcal{N}$  represents the number of degrees of freedom of our system. We collect a set of  $N_t$  equispaced snapshots  $\{x_i\}_{i=1}^{N_t}$  and we arrange them by column in two matrices,  $X$  and  $X'$ , where  $X'$  is the time-shifted version of  $X$ . We also collect the input control snapshots  $\{\eta_i\}_{i=1}^{N_t-1}$ , with  $\eta_i \in \mathbb{R}^{\mathcal{L}}$ , in the matrix  $\Upsilon$ , obtaining the following matrices:

$$X = \begin{bmatrix} | & | & & | \\ x_1 & x_2 & \dots & x_{N_t-1} \\ | & | & & | \end{bmatrix}, \quad X' = \begin{bmatrix} | & | & & | \\ x_2 & x_3 & \dots & x_{N_t} \\ | & | & & | \end{bmatrix}, \quad \Upsilon = \begin{bmatrix} | & | & & | \\ \eta_1 & \eta_2 & \dots & \eta_{N_t-1} \\ | & | & & | \end{bmatrix}.$$

We remark that the snapshots can represent data coming from experiments, from simulations, or even sensors and acquired in real-time.

DMDC is a regression-based approach to system identification that is able to disambiguate the intrinsic dynamics, described by the matrix  $A$ , and the effects of control, described by the matrix  $B$ , as in the following

$$X' \approx AX + B\Upsilon = \begin{bmatrix} A & B \end{bmatrix} \begin{bmatrix} X \\ \Upsilon \end{bmatrix} := G\Xi. \quad (4)$$

We seek an approximation of the linear mappings  $A$  and  $B$  using only the three data matrices. We start by computing the SVD of the matrix  $\Xi$  in 4, which contains both the state and control snapshot information, as  $\Xi \approx U\Sigma V^*$ . With the symbol  $*$  we denote the conjugate transpose, and we truncate the SVD keeping only the first  $r_\Xi$  modes. We can thus express the best-fit matrix  $G \in \mathbb{R}^{N \times (N+\mathcal{L})}$  as  $G \approx X'\Xi^{-1} = X'V\Sigma^{-1}U^*$ . By rewriting  $U^* = [U_1^* \ U_2^*]$ , and by computing the SVD of the output matrix  $X' \approx U_{X'}\Sigma_{X'}V_{X'}^*$ , we can compute the reduced order approximation of  $A$  and  $B$  as

$$\tilde{A} = U_{X'}^* X' V \Sigma^{-1} U_1^* U_{X'}, \quad (5)$$

$$\tilde{B} = U_{X'}^* X' V \Sigma^{-1} U_2^*. \quad (6)$$

We remark that the truncation rank  $r_{X'}$  of the SVD of the output matrix has to be less or equal to  $r_\Xi$ . With this reduced order operators we can write  $\tilde{x}_{k+1} = \tilde{A}\tilde{x}_k + \tilde{B}\eta_k$ , where  $\tilde{x}_k = U_{X'}x_k$ . The dynamic modes of  $A$  can be computed from the eigenvectors  $w$  of  $\tilde{A}$  as  $\phi = X'V\Sigma^{-1}U_1^*U_{X'}w$ .

## 4 A partitioned approach for time-dependent OCPs

In this section we are going to explain how to handle OCPs with DMDC. Our goal is to characterize the relationship between the current measurements of the time-dependent OCP  $x_k$ , the future one  $x_{k+1}$ , and the current input  $\eta_k$ , given by the desired state  $y_d$  at each time instant  $t_k$  for a finite number of steps  $k = 1, \dots, N_t$ :  $x_{k+1} = Ax_k + B\eta_k, \forall k = 1, \dots, N_t - 1$ . We remark that the current input for our OCP system is the desired state  $y_d$ . In fact, it represents the target state that we want to achieve and hence all the OCP variables (state, control, and adjoint) depend on it. Due to such a dependency, a modification in the desired state will cause a change in the other variables. We present a *partitioned approach* in order to identify two separate dynamical systems: one for the state, and one for the adjoint variables. The control can then be reconstructed through  $\alpha$  and the adjoint variable by using the linear relation in (3). For the state variable, we use as measurement matrices  $X_y \in \mathbb{R}^{N_y \times (N_t-1)}$  and  $X'_y \in \mathbb{R}^{N_y \times (N_t-1)}$  given by:

$$X_y = \begin{bmatrix} | & | & & | \\ y_1 & y_2 & \dots & y_{N_t-1} \\ | & | & & | \end{bmatrix}, \quad X'_y = \begin{bmatrix} | & | & & | \\ y_2 & y_3 & \dots & y_{N_t} \\ | & | & & | \end{bmatrix}, \quad (7)$$

where each row represents the time series of the state measurement for a particular spatial point given by the space-time discretization. On the other hand, each column contains the coefficients of the FE expansion of the state space-time variable. The final model we obtain is:

$$X'_y = A_y X_y + B_y \Upsilon_d. \quad (8)$$

For the adjoint variable we have that  $X_z \in \mathbb{R}^{N_y \times (N_t-1)}$ ,  $X'_z \in \mathbb{R}^{N_y \times (N_t-1)}$  where each row represents the time series of the adjoint measurement and each column collects the coefficients of the FE expansion of the adjoint space-time variable. We obtain the DMDC model as:

$$X'_z = A_z X_z + B_z \Upsilon_d. \quad (9)$$

We emphasize that the input matrix  $\Upsilon_d$  is the same for all the models.

## 5 Numerical results

In this section, we present the numerical results to validate the DMDC approach applied to OCPs. The first example takes into consideration an unsteady Graetz Flow boundary OCP. A second test case deals with a time-dependent OCP governed by Stokes equations. The experiments validate the performances of DMDC strategy in term of reconstruction and prediction. Indeed, we define the time-pointwise relative error  $E_k$  as:

$$E_k = \|x_k - \tilde{x}_k\|_2 / \|x_k\|_2, \quad (10)$$

where  $x_k$  represents the generic true snapshot at time  $t_k$ , and  $\tilde{x}_k$  the approximated variable. This error is shown for the reconstruction analysis. For the prediction, we average (10) over

all the time instances in the test data set. We vary the size of the training data set and we keep fixed 20 as dimension for the test data set, to understand sensitivity of the method with respect to the data needed for an accurate prediction. For the computations we used the following libraries: multiphenics [1], which is an implementation in FEniCS [22] for block-based systems, and PyDMD [11].

## 5.1 Boundary OCP governed by a Graetz Flow

Let us consider a boundary control governed by a Graetz Flow in the time interval  $[0, T] = [0, 1]$  and in the rectangular space domain  $\Omega = [0, 3] \times [0, 1] \in \mathbb{R}^2$  as depicted in Figure 1. The control domain

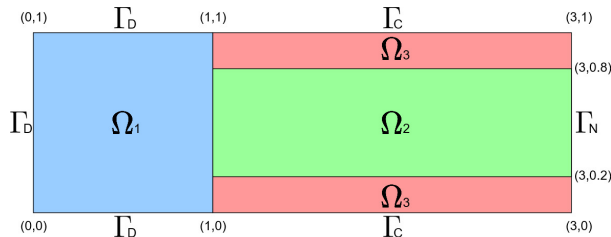


Figure 1: *Graetz Flow*: space domain.

is  $\Gamma_C = ([1, 3] \times \{0\}) \cup ([1, 3] \times \{1\})$ , while the observation domain is  $([1, 3] \times [0, 0.2]) \cup ([1, 3] \times [0.8, 1])$ . The Neumann conditions are applied to  $\Gamma_N = \{3\} \times [0, 1]$  and  $\Gamma_D = \partial\Omega \setminus (\Gamma_C \cup \Gamma_N)$ . We recall that  $Y = H_{\Gamma_D}^1(\Omega)$ , i.e. the set of functions that are  $H^1$  in the domain but null on  $\Gamma_D$ , and the control space  $U = L^2(\Gamma_C)$ . We recall that we can recover an homogeneous problem of the form presented in section 2 after a lifting procedure [27]. Thus, the Lagrangian formulation of this OCP reads: find  $(y, u) \in \mathcal{Y}_0 \times \mathcal{U}$  which solves:

$$\min_{(y,u) \in \mathcal{Y}_0 \times \mathcal{U}} J(y, u) = \frac{1}{2} \int_0^T \int_{\Omega_3} (y - y_d)^2 dx dt + \frac{\alpha}{2} \int_0^T \int_{\Gamma_C} u^2 ds dt \quad (11)$$

constrained to

$$\begin{cases} y_t - \epsilon \Delta y + \beta \cdot \nabla y = 0 & \text{in } \Omega \times (0, T), \\ y = 1 & \text{on } \Gamma_D \times (0, T), \\ \epsilon \frac{\partial y}{\partial n} = u & \text{on } \Gamma_C \times (0, T), \\ \epsilon \frac{\partial y}{\partial n} = 0 & \text{on } \Gamma_N \times (0, T), \\ y = y_0 & \text{in } \Omega \times \{0\}, \end{cases} \quad (12)$$

where  $\epsilon = \frac{1}{12}$ , the vector field  $\beta$  is defined as  $[x_2(1 - x_2), 0]$ , and  $x_2$  as vertical spatial coordinate. The desired state profile is  $y_d = 1 + t$ ,  $\alpha = 10^{-2}$  is a penalization parameter on the control, and  $y_0$  is a null function verifying the boundary conditions. For the discretization, we employed  $\mathbb{P}^1$  elements for all the variables with  $\mathcal{N}_y = \mathcal{N}_u = 2304$ . Moreover, in terms of time discretization, we consider  $\Delta t = 0.02$ , leading to  $N_t = 50$  time instances for the time interval  $[0, 1]$ . Thus, the global space-time dimension is 345600. In the left panel of Figure 2 we plotted the relative reconstruction error  $E_k$  for all the variables of interest and for every  $k = 1, \dots, 50$ . We used 4 DMD modes for the state and 3 for the adjoint. The mean relative error for the state is 1.3%, while for the adjoint variable is 3.2%.

In Figure 2 (right panel) we plotted the  $L^2$  mean relative prediction error over 20 future states for the state, and adjoint variable, varying the dimension of the train dataset. We see that for the state variable we need at least 20 snapshots in order to have a satisfactory prediction accuracy below 4%, while for the adjoint variable 10 snapshots are sufficient.

## 5.2 OCP governed by time-dependent Stokes Equations

We now deal with a distributed control problem governed by time-dependent Stokes equation. Let us consider the spatial domain  $\Omega$  as the unit square in  $\mathbb{R}^2$  and the time interval  $[0, 1]$ . For this

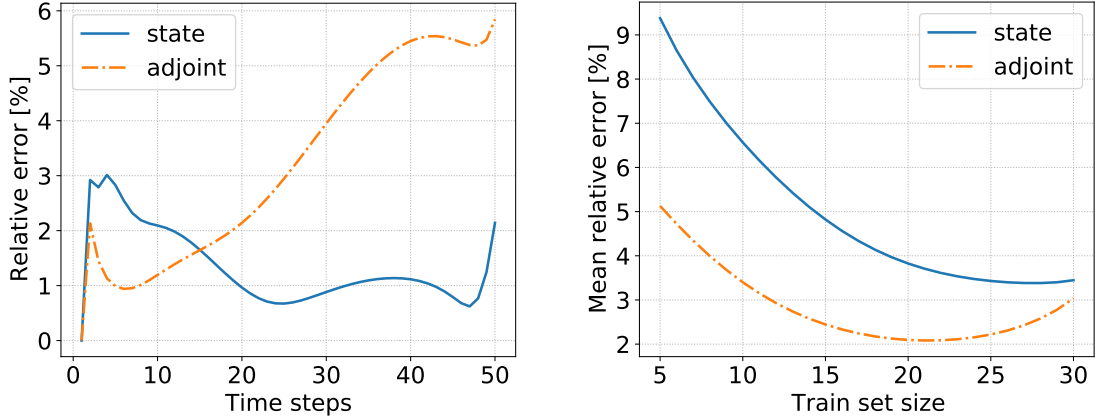


Figure 2: On the left the  $L^2$  relative reconstruction error for the Graetz case for state and adjoint variables. On the right the  $L^2$  mean relative prediction error. The average is done over 20 snapshots in the future.

specific case  $\Gamma_D = \partial\Omega$ , and we consider

$$\mathcal{V}_0 \doteq \{v \in L^2(0, T; V) \text{ such that } v_t \in L^2(0, T; V^*) \text{ such that } v(0) = 0\}$$

with  $V \doteq [H_{\Gamma_D}^1(\Omega)]^2$  and  $\mathcal{P} = L^2(0, T; L_0^2(\Omega))$ , where  $L_0^2(\Omega)$  is the space of functions that have null mean over  $\Omega$  with  $L^2$  regularity<sup>1</sup>. We seek the state-control variable in  $\mathcal{Y}_0 \times \mathcal{U}$  where  $\mathcal{Y}_0 = \mathcal{V}_0 \times \mathcal{P}$  and  $\mathcal{U} = [L^2(\Omega)]^2$ . The specific problem we are dealing with is to find the minimum of

$$\min_{((v,p),u) \in \mathcal{Y}_0 \times \mathcal{U}} J(((v,p),u)) := \frac{1}{2} \int_0^T \int_{\Omega} (v - v_d)^2 dx dt + \frac{\alpha}{2} \int_0^T \int_{\Omega} u^2 dx dt, \quad (14)$$

constrained to the equations:

$$\begin{cases} v_t - \Delta v + \nabla p = u & \text{in } \Omega \times (0, T), \\ -\nabla \cdot v = 0 & \text{in } \Omega \times (0, T), \\ v = 0 & \text{on } \partial\Omega \times (0, T), \\ v(0) = 0 & \text{in } \Omega \times \{0\}, \end{cases} \quad (15)$$

where  $v_d = [10(1+t) (1 + \frac{1}{2} \cos(4\pi t - \pi)), 0] \in L^2(0, T; [L^2(\Omega)]^2)$  is considered on the whole space-time domain, and  $\alpha = 10^{-5}$ . For the space discretization we employed  $\mathbb{P}^2 - \mathbb{P}^1$  polynomials for the velocity and pressure fields both for the state and the adjoint variables, while for the control we used  $\mathbb{P}^2$  polynomials. Thus, the FE dimension is 674 for state/adjoint velocity and control variables, while it is 337 for the state and adjoint pressure. In terms of time discretization, in the interval  $[0, 1]$  we considered  $N_t = 50$  time instances, with  $\Delta t = 0.02$ . The final dimension of the system is 134800. In the left panel of Figure 3 we plotted the relative reconstruction error  $E_k$  for all the variables of interest and for every  $k = 1, \dots, 50$ . The error at the first time step is exactly 0, while the spike at the last time instant is due to the nature of DMD which divides the snapshots data into two shifted matrices and we have the accumulation of all the residuals. The maximum error is registered for the adjoint velocity and it is below 1.5%, while on average all the variables present an error below 0.6%. We remark that the adjoint pressure snapshots have been normalized removing the mean of all the states before applying the DMDc. Even if such preprocessing can be done only for reconstruction, we emphasize that the adjoint pressure in this case is not a variable of interest for prediction purposes since only the adjoint velocity affects the control in the optimality equation. Nonetheless we present its relative reconstruction error in order to show that the partitioned approach is able to deal also with such variable.

<sup>1</sup>Numerically, to enforce the condition of null mean for the state pressure variable, we employed Lagrange multipliers. Namely, the condition is weakly imposed in integral form

$$\int_{\Omega} p \lambda dx = 0, \quad \forall \lambda \in \mathbb{R}. \quad (13)$$

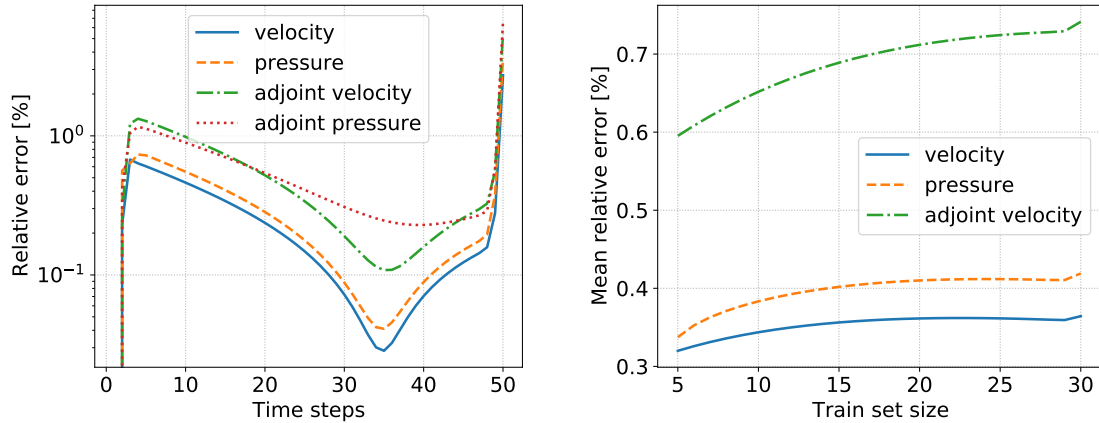


Figure 3: On the left the  $L^2$  relative reconstruction error for the Stokes case for velocity, pressure, and the adjoint variables. On the right the  $L^2$  mean relative prediction error. The average is done over 20 snapshots in the future.

In Figure 3 (right panel) we plotted the  $L^2$  mean relative prediction error over 20 future states for velocity, pressure, and adjoint velocity, varying the dimension of the train dataset. We notice an almost stationary behaviour of the mean error for all the variables of interest, with all the values below 0.8%. This suggests that the future state prediction is robust with respect to the amount of available data.

## 6 Conclusions and perspectives

In this work we showed the potential of data-driven methods for the resolution of time-dependent optimal control problems with PDE constraints. A further improvement of the work might concern a deeper analysis of the sensitivity of the problems with respect to the penalization parameter  $\alpha$  which drastically changes the magnitude of the adjoint variable. Another possible approach could be to use the data-driven sparse identification of nonlinear dynamics with control method [6], instead of DMDC. Lastly, we stress that even if the test cases are quite academic, we believe in the potential of such an approach in more complex setting based on data collection. Indeed, this represents a first attempt a deeper study of this formulation, which might be of interest in many interdisciplinary research fields.

## Acknowledgements

This work was partially funded by European Union Funding for Research and Innovation — Horizon 2020 Program — in the framework of European Research Council Executive Agency: H2020 ERC CoG 2015 AROMA-CFD project 681447 “Advanced Reduced Order Methods with Applications in Computational Fluid Dynamics” P.I. Professor Gianluigi Rozza.

## References

- [1] multiphenics - easy prototyping of multiphysics problems in fenics, <https://mathlab.sissa.it/multiphenics>.
- [2] Z. Bai, E. Kaiser, J. L. Proctor, J. N. Kutz, and S. L. Brunton. Dynamic mode decomposition for compressive system identification. *AIAA Journal*, 58(2):561–574, 2020. doi:10.2514/1.J057870.

---

This constraint reflects in the derivation of the adjoint equation and an extra term appears in the divergence free constraint in weak form.

- [3] F. Ballarin, E. Faggiano, A. Manzoni, A. Quarteroni, G. Rozza, S. Ippolito, C. Antona, and R. Scrofani. Numerical modeling of hemodynamics scenarios of patient-specific coronary artery bypass grafts. *Biomechanics and Modeling in Mechanobiology*, 16(4):1373–1399, Aug 2017. doi:10.1007/s10237-017-0893-7.
- [4] M. Benzi, G. H. Golub, and J. Liesen. Numerical solution of saddle point problems. *Acta Numerica*, 14:1–137, 2005. doi:10.1017/S0962492904000212.
- [5] S. L. Brunton and J. N. Kutz. *Data-Driven Science and Engineering: Machine Learning, Dynamical Systems, and Control*. Cambridge University Press, 2019.
- [6] S. L. Brunton, J. L. Proctor, and J. N. Kutz. Sparse identification of nonlinear dynamics with control (SINDYc). *IFAC-PapersOnLine*, 49(18):710–715, 2016. doi:10.1016/j.ifacol.2016.10.249.
- [7] L. Dedè. Optimal flow control for Navier-Stokes equations: Drag minimization. *International Journal for Numerical Methods in Fluids*, 55(4):347–366, 2007.
- [8] L. Dedè. Reduced basis method and a posteriori error estimation for parametrized linear-quadratic optimal control problems. *SIAM Journal on Scientific Computing*, 32(2):997–1019, 2010.
- [9] M. C. Delfour and J. Zolésio. *Shapes and geometries: metrics, analysis, differential calculus, and optimization*, volume 22. SIAM, Philadelphia, 2011. doi:10.1137/1.9780898719826.
- [10] N. Demo, M. Tezzele, G. Gustin, G. Lavini, and G. Rozza. Shape optimization by means of proper orthogonal decomposition and dynamic mode decomposition. In *Technology and Science for the Ships of the Future: Proceedings of NAV 2018: 19th International Conference on Ship & Maritime Research*, pages 212–219. IOS Press, 2018. doi:10.3233/978-1-61499-870-9-212.
- [11] N. Demo, M. Tezzele, and G. Rozza. PyDMD: Python Dynamic Mode Decomposition. *The Journal of Open Source Software*, 3(22):530, 2018. doi:https://doi.org/10.21105/joss.00530.
- [12] S. Glas, A. Mayerhofer, and K. Urban. *Two Ways to Treat Time in Reduced Basis Methods*, pages 1–16. Springer International Publishing, Cham, 2017. doi:10.1007/978-3-319-58786-8\_1.
- [13] A. Goldschmidt, E. Kaiser, J. L. Dubois, S. L. Brunton, and J. N. Kutz. Bilinear dynamic mode decomposition for quantum control. *New Journal of Physics*, 23(3):033035, 2021. doi:10.1088/1367-2630/abe972.
- [14] J. Haslinger and R. A. E. Mäkinen. *Introduction to shape optimization: theory, approximation, and computation*. Advances in Design and Control. SIAM, Philadelphia, 2003. doi:10.1137/1.9780898718690.
- [15] M. Hinze, M. Köster, and S. Turek. A hierarchical space-time solver for distributed control of the Stokes equation. *Technical Report, SPP1253-16-01*, 2008.
- [16] M. Hinze, M. Köster, and S. Turek. A space-time multigrid method for optimal flow control. In *Constrained optimization and optimal control for partial differential equations*, page 147. Springer, 2012. doi:10.1007/978-3-0348-0133-1\_8.
- [17] M. Hinze, R. Pinnau, M. Ulbrich, and S. Ulbrich. *Optimization with PDE constraints*, volume 23 of *Mathematical Modelling: Theory and Applications*. Springer Netherlands, 2009. doi:10.1007/978-1-4020-8839-1.
- [18] L. Iapichino, S. Trenz, and S. Volkwein. Reduced-order multiobjective optimal control of semi-linear parabolic problems. In B. Karasözen, M. Manguoğlu, M. Tezer-Sezgin, S. Göktepe, and Ö. Uğur, editors, *Numerical Mathematics and Advanced Applications ENUMATH 2015*, pages 389–397, Cham, 2016. Springer International Publishing. doi:10.1007/978-3-319-39929-4\_37.



- [19] J. N. Kutz, S. L. Brunton, B. W. Brunton, and J. L. Proctor. *Dynamic Mode Decomposition: Data-Driven Modeling of Complex Systems*. SIAM, 2016. doi:10.1137/1.9781611974508.
- [20] T. Lassila, A. Manzoni, A. Quarteroni, and G. Rozza. A reduced computational and geometrical framework for inverse problems in hemodynamics. *International Journal for Numerical Methods in Biomedical Engineering*, 29(7):741–776, 2013. doi:10.1002/cnm.2559.
- [21] G. Leugering, P. Benner, S. Engell, A. Griewank, H. Harbrecht, M. Hinze, R. Rannacher, and S. Ulbrich. *Trends in PDE constrained optimization*, volume 165 of *International Series of Numerical Mathematics*. Springer, New York, 2014. doi:10.1007/978-3-319-05083-6.
- [22] A. Logg, K. Mardal, and G. Wells. *Automated Solution of Differential Equations by the Finite Element Method*. Springer-Verlag, Berlin, 2012.
- [23] B. Mohammadi and O. Pironneau. *Applied shape optimization for fluids*. Oxford University Press, New York, 2010.
- [24] A. Narasingam and J. S.-I. Kwon. Development of local dynamic mode decomposition with control: Application to model predictive control of hydraulic fracturing. *Computers & Chemical Engineering*, 106:501–511, 2017. doi:10.1016/j.compchemeng.2017.07.002.
- [25] F. Negri, A. Manzoni, and G. Rozza. Reduced basis approximation of parametrized optimal flow control problems for the Stokes equations. *Computers & Mathematics with Applications*, 69(4):319–336, 2015.
- [26] J. L. Proctor, S. L. Brunton, and J. N. Kutz. Dynamic Mode Decomposition with Control. *SIAM Journal on Applied Dynamical Systems*, 15(1):142–161, 2016. doi:10.1137/15M1013857.
- [27] A. Quarteroni, G. Rozza, L. Dedè, and A. Quaini. Numerical approximation of a control problem for advection-diffusion processes. In *Ceragioli F., Dontchev A., Futura H., Marti K., Pandolfi L. (eds) System Modeling and Optimization. International Federation for Information Processing, CSMO Conference on System Modeling and Optimization*, pages vol 199, 261–273. Springer, Boston, 2005.
- [28] A. Quarteroni, G. Rozza, and A. Quaini. Reduced basis methods for optimal control of advection-diffusion problems. In *Advances in Numerical Mathematics*, number 2006-003 in CMCS-CONF, pages 193–216. RAS and University of Houston, 2007.
- [29] G. Rozza, M. Hess, G. Stabile, M. Tezzele, and F. Ballarin. Basic Ideas and Tools for Projection-Based Model Reduction of Parametric Partial Differential Equations. In P. Benner, S. Grivet-Talocia, A. Quarteroni, G. Rozza, W. H. A. Schilders, and L. M. Silveira, editors, *Model Order Reduction*, volume 2, chapter 1, pages 1–47. De Gruyter, Berlin, Boston, 2020. doi:10.1515/9783110671490-001.
- [30] J. Schöberl and W. Zulehner. Symmetric indefinite preconditioners for saddle point problems with applications to PDE-constrained optimisation problems. *SIAM Journal on Matrix Analysis and Applications*, 29(3):752–773, 2007. doi:10.1137/060660977.
- [31] Z. K. Seymen, H. Yücel, and B. Karasözen. Distributed optimal control of time-dependent diffusion–convection–reaction equations using space–time discretization. *Journal of Computational and Applied Mathematics*, 261:146–157, 2014. doi:10.1016/j.cam.2013.11.006.
- [32] M. Stoll and A. Wathen. All-at-once solution of time-dependent Stokes control. *J. Comput. Phys.*, 232(1):498–515, Jan. 2013. doi:10.1016/j.jcp.2012.08.039.
- [33] M. Strazzullo, F. Ballarin, R. Mosetti, and G. Rozza. Model reduction for parametrized optimal control problems in environmental marine sciences and engineering. *SIAM Journal on Scientific Computing*, 40(4):B1055–B1079, 2018. doi:10.1137/17M1150591.
- [34] M. Strazzullo, F. Ballarin, and G. Rozza. POD-Galerkin Model Order Reduction for Parametrized Time Dependent Linear Quadratic Optimal Control Problems in Saddle Point Formulation. *Journal of Scientific Computing*, 83(55), 2020. doi:10.1007/s10915-020-01232-x.

- [35] M. Strazzullo, F. Ballarin, and G. Rozza. POD-Galerkin model order reduction for parametrized nonlinear time dependent optimal flow control: an application to Shallow Water Equations. to appear in *Journal of Numerical Mathematics*, 2021, <https://arxiv.org/abs/2003.09695>.
- [36] M. Strazzullo, F. Ballarin, and G. Rozza. A Certified Reduced Basis method for linear parametrized parabolic optimal control problems in space-time formulation. Submitted, 2021, <https://arxiv.org/abs/2103.00460>.
- [37] M. Strazzullo, Z. Zainib, F. Ballarin, and G. Rozza. Reduced order methods for parametrized nonlinear and time dependent optimal flow control problems: towards applications in biomedical and environmental sciences. *Numerical Mathematics and Advanced Applications ENU-MATH 2019*, 2021.
- [38] M. Tezzele, N. Demo, A. Mola, and G. Rozza. An integrated data-driven computational pipeline with model order reduction for industrial and applied mathematics. *Special Volume ECMI, In Press*, 2021.
- [39] M. Tezzele, N. Demo, G. Stabile, A. Mola, and G. Rozza. Enhancing CFD predictions in shape design problems by model and parameter space reduction. *Advanced Modeling and Simulation in Engineering Sciences*, 7(40), 2020. doi:10.1186/s40323-020-00177-y.
- [40] F. Tröltzsch. Optimal Control of Partial Differential Equations. *Graduate Studies in Mathematics*, 112, 2010.
- [41] K. Urban and A. T. Patera. A new error bound for reduced basis approximation of parabolic partial differential equations. *Comptes Rendus Mathématique*, 350(3-4):203–207, 2012. doi:10.1016/j.crma.2012.01.026.
- [42] M. Yano. A space-time Petrov–Galerkin certified reduced basis method: Application to the Boussinesq equations. *SIAM Journal on Scientific Computing*, 36(1):A232–A266, 2014. doi:10.1137/120903300.
- [43] M. Yano, A. T. Patera, and K. Urban. A space-time hp-interpolation-based certified reduced basis method for Burgers’ equation. *Mathematical Models and Methods in Applied Sciences*, 24(09):1903–1935, 2014. doi:10.1142/S0218202514500110.
- [44] Z. Zainib, F. Ballarin, S. Frenes, P. Triverio, L. Jiménez-Juan, and G. Rozza. Reduced order methods for parametric optimal flow control in coronary bypass grafts, toward patient-specific data assimilation. *International Journal for Numerical Methods in Biomedical Engineering*, page e3367, 2020. doi:10.1002/cnm.3367.